# Hall Coefficient of Semimetals

Abhisek Samanta,[1,*] Daniel P. Arovas,[2,†] and Assa Auerbach[1,‡]
[1]Physics Department, Technion, Haifa 32000, Israel
[2]Department of Physics, University of California at San Diego, La Jolla, California 92093, USA

(Received 24 September 2020; accepted 21 January 2021; published 19 February 2021)

A recently developed formula for the Hall coefficient [A. Auerbach, Phys. Rev. Lett. **121**, 066601 (2018)] is applied to nodal line and Weyl semimetals (including graphene) and to spin-orbit split semiconductor bands in two and three dimensions. The calculation reduces to a ratio of two equilibrium susceptibilities, where corrections are negligible at weak disorder. Deviations from Drude's inverse carrier density are associated with band degeneracies, Fermi surface topology, and interband currents. Experiments which can measure these deviations are proposed.

DOI: 10.1103/PhysRevLett.126.076603

Semimetals are characterized by proximity of the Fermi energy to band degeneracies. Vigorous research has recently been invested in semimetals on surfaces of topological insulators [1,2], Dirac and Weyl semimetals [3–8], and on semimetal platforms for Majorana state applications [9].

This Letter focuses on the Hall coefficient of semimetals, which has been traditionally used to measure the charge carrier density $n$ using Drude's relation $R_H \propto n^{-1}$. In semimetals, Drude's relation may break down due to multiband effects and Fermi surface topology. For example, corrections to Drude's relation was found by Liu *et al.* [10] for spin-orbit split semiconductor bands. Multiband conductivity calculations involve coupled Boltzmann equations with interband collision integrals which are quite challenging [11,12].

We can avoid coupled Boltzmann equations by applying the Hall coefficient formula [13,14] to multiband Hamiltonians. The dissipative scattering rates drop out, and $R_H$ is primarily determined by the nondissipative Lorentz force captured by the current-magnetization-current (CMC) susceptibility $\chi_{\mathsf{CMC}}$, and the conductivity sum rule (CSR) $\chi_{\mathsf{CSR}}$. Both coefficients are nondissipative: the CMC describes the effect of the Lorentz force on the currents, and the CSR governs their reactive response.

Crucial to our approach is the estimation of the formula's correction term $\mathcal{R}^{\text{corr}}$, which is determined by higher moments of the dynamical conductivity. This Letter shows that in the "good quasiparticles" (Boltzmann) regime, $\mathcal{R}^{\text{corr}}$ can be neglected for disorder strength less than the Fermi energy.

Our key results are (i) For Weyl point semimetals in two and three dimensions (including graphene), the intraband $R_H^{\mathsf{INTRA}}(n)$ exhibits a Drude-like divergence, which is cut off by interband scattering at low densities. (ii) The nodal line semimetal (see Fig. 1) exhibits a constant (rather than diverging) Hall coefficient, with a sign change at the nodal energy. (iii) Previous results [10] of spin-orbit split bands are extended into the interband transport regime, and to three dimensions. (iv) $\mathcal{R}^{\text{corr}}$ is shown to be relatively suppressed by the disorder potential fluctuations divided by the Fermi energy squared. The Letter ends with a summary and proposals for experiments.

The Hall coefficient formula, as derived directly from the Kubo formulas [13,14], for any Hamiltonian $\mathcal{H}$ and spectrum $\{E_n, |n\rangle\}$,

$$R_H \equiv \lim_{B\to 0}\left(\sigma_{xx}^{-2}\frac{\partial\sigma_{xy}}{\partial B}\right) = \frac{\chi_{\mathsf{CMC}}}{\chi_{\mathsf{CSR}}^2} + \mathcal{R}^{\text{corr}}. \tag{1}$$

$\sigma_{\alpha\beta}$ is the conductivity tensor (assuming $C4$ symmetry) and $B$ is the magnetic field in the $z$ direction. $\chi_{\mathsf{CMC}} = \mathrm{Im}\langle j^y, [M, j^x]\rangle - \mathrm{Im}\langle j^x, [M, j^y]\rangle$ and $\chi_{\mathsf{CSR}} = \langle j^x, j^x\rangle$,

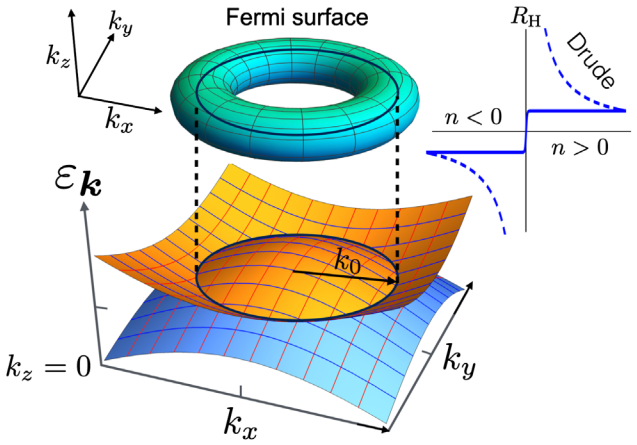


FIG. 1. Nodal line semimetal. The nodal line is marked by the black circle of radius $k_0$. The three dimensional toroidal Fermi surface (top) is depicted. At the upper right corner, the qualitative behavior of the Hall coefficient (solid line) is compared to Drude relation for density $n$ as measured from the nodal circle filling.

 

where $j^\alpha$ is the uniform current in the $\alpha$ direction, and $M = \partial\mathcal{H}/\partial B$ is the diamagnetization operator. The inner products are defined by equilibrium susceptibilities, [15]

$$(j^\alpha, A) = \frac{1}{Z}\sum_{nm}\frac{e^{-\beta E_n} - e^{-\beta E_m}}{E_m - E_n}\langle n|j^\alpha|m\rangle\langle m|A|n\rangle, \quad (2)$$

where $Z = \mathrm{Tr}e^{-\beta\mathcal{H}}$ and $\beta$ is the inverse temperature.

The correction term $\mathcal{R}^{\mathrm{corr}}$ is given by

$$\mathcal{R}^{\mathrm{corr}} = \frac{1}{\chi_{\mathsf{CSR}}}\sum_{i,j=0}^{\infty}(1-\delta_{i,0}\delta_{j,0})\mathcal{M}''_{2i,2j} \times\prod_{i'=0}^{i}\left(-\frac{\Delta_{2i'-1}}{\Delta_{2i'}}\right)\prod_{j'=0}^{j}\left(-\frac{\Delta_{2j'-1}}{\Delta_{2j'}}\right). \quad (3)$$

$\mathcal{M}''_{2i,2j}$ are cross susceptibilities, defined by the matrix elements of the magnetization commutator $[M,\bullet]$ between two currents' Krylov bases. The Krylov bases are generated by orthonormalizing the sets of operators $[\mathcal{H},[\cdots,[\mathcal{H},j^\alpha]]]$. $\Delta_{i'}$ are the conductivity recurrent [16], which can be obtained from the conductivity moments, defined by $\mu_{2i} = \langle[j^x,[\mathcal{H},[\cdots,[\mathcal{H},j^x]]]]\rangle$, where $\mathcal{H}$ appears $2i-1$ times. Instructions for calculating $\mathcal{M}''_{2i,2j}$ and $\Delta_{i'}$ are reviewed in [15]. Physically, $\mathcal{R}^{\mathrm{corr}}$ incorporates the higher order effects of current nonconservation. In several examples, its relative magnitude can be suppressed by using a renormalized Hamiltonian [14]. Later, we estimate $\mathcal{R}^{\mathrm{corr}}$ and show that it can be neglected in regimes of weak disorder which concern this Letter.

We consider a general two-band Hamiltonian

$$\mathcal{H}_0 \equiv \sum_{\boldsymbol{k}}\sum_{l,l'=1}^{2} c^\dagger_{l\boldsymbol{k}}h_{ll'}(\boldsymbol{k})c_{l'\boldsymbol{k}}. \quad (4)$$

where $c^\dagger_{l\boldsymbol{k}}$ creates a Bloch electron on band $l$ and wave vector $\boldsymbol{k}$. A random potential with fluctuation $V^2_{\mathrm{dis}}$ introduces a transport scattering rate $\hbar/\tau_{\mathrm{tr}} \sim V^2_{\mathrm{dis}}/|\varepsilon_F|$, where $\varepsilon_F$ is the Fermi energy measured from the nearest particle-hole symmetric energy or band extremum.

Within the good quasiparticles regime, $\hbar/\tau_{\mathrm{tr}} \ll \varepsilon_F$, the ratio of the disorder strength to interband gap at the Fermi energy $\Delta\varepsilon$, defines two distinct transport regimes. Importantly, for evaluation of Eq. (1), we have the freedom to choose the (renormalized) effective Hamiltonian which best describes the low energy correlations. Our choice determines the values of $\chi_{\mathsf{CMC}}$, $\chi_{\mathsf{CSR}}$, and $\mathcal{R}^{\mathrm{corr}}$. It is the latter we wish to minimize.

(i) Intraband regime applies for $V^2_{\mathrm{dis}} \ll (\Delta\varepsilon)^2$, where interband scattering is suppressed, and transport is dominated by band-diagonal current and magnetization operators

$$j^\alpha_{\mathsf{INTRA}} = e\sum_{i,\boldsymbol{k}} c^\dagger_{i\boldsymbol{k}}v^\alpha_i(\boldsymbol{k})c_{i\boldsymbol{k}}, \qquad \alpha = x,y, \quad i = 1,2,$$
$$M_{\mathsf{INTRA}} = \frac{ie}{2c}\sum_{i,\boldsymbol{k}} c^\dagger_{i\boldsymbol{k}}\left(v^y_i(\boldsymbol{k})\frac{\partial}{\partial k_x} - v^x_i(\boldsymbol{k})\frac{\partial}{\partial k_y}\right)c_{i\boldsymbol{k}}, \quad (5)$$

with $v^\alpha_i(\boldsymbol{k}) = \partial\varepsilon_i(\boldsymbol{k})/\partial k_\alpha$, where $\varepsilon_i(\boldsymbol{k})$ $(i = 1, 2)$ are the eigenvalues of $h_{ll'}(\boldsymbol{k})$. The susceptibilities in this regime are [15]

$$\chi^{\mathsf{INTRA}}_{\mathsf{CMC}} = \frac{e^3}{c}\sum_{i=1}^{2}\int\frac{d^dk}{(2\pi)^d}F_i(\boldsymbol{k})\left(-\frac{\partial f}{\partial\varepsilon}\right)_{\varepsilon=\varepsilon_i(\boldsymbol{k})},$$
$$F_i(\boldsymbol{k}) = [v^y_i(\boldsymbol{k})]^2\frac{\partial v^x_i(\boldsymbol{k})}{\partial k_x} - v^x_i(\boldsymbol{k})v^y_i(\boldsymbol{k})\frac{\partial v^y_i(\boldsymbol{k})}{\partial k_x},$$
$$\chi^{\mathsf{INTRA}}_{\mathsf{CSR}} = e^2\sum_{i=1}^{2}\int\frac{d^dk}{(2\pi)^d}(v^x_i(\boldsymbol{k}))^2\left(-\frac{\partial f}{\partial\varepsilon}\right)_{\varepsilon=\varepsilon_i(\boldsymbol{k})}. \quad (6)$$

$f_i$ is the Fermi-Dirac distribution of band $\varepsilon_i(\boldsymbol{k})$ at temperature $T$ and chemical potential $\varepsilon_F$. For any spherically symmetric band, $\varepsilon(\boldsymbol{k}) = \varepsilon(k)$, Drude's relation holds, i.e., $R_H = \chi_{\mathsf{CMC}}/\chi^2_{\mathsf{CSR}} = 1/(nec)$ [17]. For more general band structures, Eqs. (6) recover the venerable Boltzmann equation result in the "isotropic scattering limit" [18,19].

(ii) Interband regime applies within the range $(\Delta\varepsilon)^2 \le V^2_{\mathrm{dis}} \ll \varepsilon^2_F$, where disorder is strong enough to mix the two bands (but still weak enough to neglect $\mathcal{R}$, see later discussion). Interband currents now contribute to the longitudinal conductivity and to $\chi_{\mathsf{CSR}}$ [11,20]. In this regime, the susceptibilities must involve full two-band operators represented by $2\times 2$ matrices

$$j^\alpha_{ll'}(\boldsymbol{k}) \equiv e\frac{\partial h_{ll'}(\boldsymbol{k})}{\partial k_\alpha},$$
$$M_{ll'}(\boldsymbol{k}) \equiv \frac{ie}{2c}\left(j^y_{ll'}(\boldsymbol{k})\frac{\partial}{\partial k_x} - j^x_{ll'}(\boldsymbol{k})\frac{\partial}{\partial k_y}\right), \quad (7)$$

which yield the interband susceptibilities which can be conveniently expressed by [15]

$$\chi^{\mathsf{INTER}}_{\mathsf{CMC}} = \int\frac{d^dk}{(2\pi)^d}\sum_{i=1}^{2}f(\varepsilon_i(\boldsymbol{k}))F^{\mathsf{INTER}}_i(\boldsymbol{k}),$$
$$F^{\mathsf{INTER}}_i(\boldsymbol{k}) = e\left[U^\dagger_{\boldsymbol{k}}\left(\frac{\partial}{\partial k_y}[M,j^x] - \frac{\partial}{\partial k_x}[M,j^y]\right)U_{\boldsymbol{k}}\right]_{ii},$$
$$\chi^{\mathsf{INTER}}_{\mathsf{CSR}} = e\int\frac{d^dk}{(2\pi)^d}\sum_{i=1}^{2}f(\varepsilon_i(\boldsymbol{k}))\left[U^\dagger_{\boldsymbol{k}}\frac{\partial j^x(\boldsymbol{k})}{\partial k_x}U_{\boldsymbol{k}}\right]_{ii}. \quad (8)$$

The unitary matrix $U_{\boldsymbol{k}}$ diagonalizes $h(\boldsymbol{k})$. We note that the operator $\partial[M,j^\alpha]/\partial k^\beta$ includes a derivative $\partial/\partial k_\alpha$ acting to the right on $U_{\boldsymbol{k}}$. This derivative captures the effect of SU(2) rotation of Bloch states inside the Fermi volume.

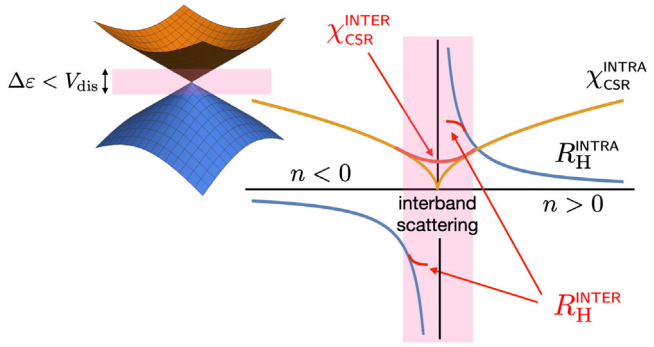


FIG. 2. The two dimensional Weyl cone, whose bands are depicted in the upper left. The intraband Hall coefficient (online, blue) and conductivity sum rule (online, orange) are plotted versus the density of carriers $n$ as measured from the nodal filling. Pink (online) regions mark the low density interband dominated transport regime, where the interband gap is lower than the disorder potential $V_{\rm dis}$. In this regime, the conductivity sum rule $\chi_{\rm CSR}^{\rm INTER}$ does not vanish at the nodal density, and the Drude-like divergence of the Hall coefficient is cut off (see text).

Now, we apply Eqs. (6) and (8) to calculate the Hall coefficients of the following models.

*Weyl semimetals.*—When the product of time reversal and inversion is not a symmetry of a system, the band structure may exhibit Weyl points, where two bands intersect at the Fermi level. Expansion of the semimetal band structure near a linear point degeneracy results in the $d$-dimensional two-band Weyl Hamiltonian [21]

$$H_0 = v_0 \boldsymbol{k}\cdot\boldsymbol{\sigma}, \tag{9}$$

which yields the conical dispersion $\varepsilon_\pm(\boldsymbol{k}) = \pm v_0|\boldsymbol{k}|$, see Fig. 2. For $d = 2$, this could describe surface states of a three dimensional topological insulator [1], or a single Dirac cone in graphene [22]. For $d = 3$, this could describe one Weyl cone in a Weyl semimetal.

The density (per cone) is $n = \mathrm{sgn}(n)k_F^d/2d\pi^{d-1}$, where $k_F$ is the Fermi wave vector. In the intraband transport regime,

$$\chi_{\rm CMC}^{\rm INTRA} = \frac{e^4 v_0^2}{c}\frac{k_F^{d-2}}{2d\pi^{d-1}}\mathrm{sgn}(n) \propto \mathrm{sgn}(n)|n|^{(d-2)/d},$$
$$\chi_{\rm CSR}^{\rm INTRA} = \frac{v_0}{2d\pi^{d-1}}k_F^{d-1} \propto |n|^{(d-1)/d}, \tag{10}$$

which recovers the Drude relation $R_H^{\rm INTRA} = 1/nec$.

For the interband regime [15], we find that

$$\chi_{\rm CMC}^{\rm INTER}(n) = \chi_{\rm CMC}^{\rm INTRA}(n), \qquad \chi_{\rm CSR}^{\rm INTER}(n) \propto n^0. \tag{11}$$

At low densities, the interband regime takes over when $\Delta\varepsilon < V_{\rm dis}$, as depicted by pink (online) shaded areas in Fig. 2. Since the sum rule in Eq. (11) does not vanish at the Weyl point, the Drude-like divergence of the Hall coefficient is cut off at the Weyl point.

Unfortunately, a quantitative calculation of $R_H^{\rm INTER}$ in this regime is not available, since the Fermi energy is half the interband gap. This violates the good quasiparticle condition, and $\mathcal{R}^{\rm corr}$ cannot be neglected (as explained later). Nevertheless, since $\chi_{\rm CSR}^{\rm INTER} > 0$, the saturation of $R_H^{\rm INTER} < \infty$ at the Weyl point still holds.

*Nodal-line semimetal.*—It is also possible for two bands to touch along a curve, as is the case in a nodal line semimetal [6,23]. Such a state of affairs has reportedly been observed in the compound ZrSiSe [24] as well as in optical lattices with ultracold fermions [25].

We consider a nodal circle of radius $k_0$ in the $k_z = 0$ plane, as depicted in Fig. 1. The dispersions near the nodal line are expanded for low values of $\delta k_\perp = \sqrt{k_x^2 + k_y^2} - k_0$ and $k_z$

$$\varepsilon_{\boldsymbol{k}\pm} \simeq \pm v_0\sqrt{\alpha^2(\delta k_\perp)^2 + k_z^2}, \tag{12}$$

where $\alpha$ is a dimensionless anisotropy parameter. Here, we limit the calculation to the intraband regime at zero temperature, where $n = k_0\varepsilon_F^2/4\pi\alpha v_0^2$. By Eq. (6), the susceptibilities are

$$\chi_{\rm CMC}^{\rm INTRA} = \frac{3e^3 v_0^2\alpha^2 n}{4k_0^2 c}, \qquad \chi_{\rm CSR}^{\rm INTRA} = e^2 v_0\left(\frac{\alpha^3 k_0 n}{16\pi}\right)^{1/2}, \tag{13}$$

which yields an unusual density dependence of the Hall coefficient

$$R_H^{\rm INTRA} = \frac{12\pi}{\alpha k_0^3 ec}\mathrm{sgn}(n). \tag{14}$$

The nodal line semimetal exhibits a density independent Hall coefficient with an abrupt sign reversal, at zero temperature and disorder. The suppression of $\chi_{\rm CMC}^{\rm INTRA}$ at large radii can be intuitively attributed to the near cancellation of the inner (holelike) and outer (electronlike) sides of the toroidal Fermi surface.

The density dependences of Weyl and nodal line semimetals are summarized in Table I.

TABLE I. Nodal line semimetal and Weyl semimetals in two and three dimensions. The density dependence of the conductivity sum rules and Hall coefficients are given for the intraband and interband transport regimes.

| Model | $\chi_{\rm CSR}^{\rm INTRA}$ | $R_H^{\rm INTRA}$ | $\chi_{\rm CSR}^{\rm INTER}$ | $R_H^{\rm INTER}$ |
|---|---|---|---|---|
| 2D Weyl | $\lvert n\rvert^{1/2}$ | $1/n$ | Const | $\leq$ const |
| 3D Weyl | $\lvert n\rvert^{2/3}$ | $1/n$ | Const | $\leq \lvert n\rvert^{1/3}$ |
| Nodal line sm | $\lvert n\rvert^{1/2}$ | $\mathrm{sgn}(n)$ | | |

*Semiconductor bands.*—Semiconductor bands with an inversion-asymmetric zinc blende structure, e.g., GaAs and CdTe, are subjected to spin orbit interactions described by the Kane and Luttinger models [26–28]. They share with semimetals the small interband gaps near the Fermi energy. We study two models: (i) The (heavy) hole bands in a two dimensional quantum well (2D$H$) [10]

$$h^{2DH}(\boldsymbol{k}) = \frac{k^2}{2m}\mathbb{I} \pm \beta[k_y(k_y^2 - 3k_x^2)\sigma^x + k_x(k_x^2 - 3k_y^2)\sigma^y], \quad (15)$$

where the Rashba parameter $\beta$ depends on the perpendicular electric field [10]. The bands $\varepsilon^{2DH}_{\boldsymbol{k}\pm} = k^2/2m \pm \beta k^3$ are rotationally symmetric, and split by $\beta$.

(ii) The conduction band in a cubic crystal, with spin orbit interaction splitting expanded up to third order in $k$ [28]

$$h^{3DC}(\boldsymbol{k}) = \frac{k^2}{2m}\mathbb{I} \pm \beta \boldsymbol{h}(\boldsymbol{k}) \cdot \boldsymbol{\sigma},$$
$$\boldsymbol{h}(\boldsymbol{k}) = (k_y^2 - k_z^2)k_x\hat{\boldsymbol{x}} + (k_z^2 - k_x^2)k_y\hat{\boldsymbol{y}} + (k_x^2 - k_y^2)k_z\hat{\boldsymbol{z}}, \quad (16)$$

the dispersions $\varepsilon^{3DC}_{\boldsymbol{k}\pm} = k^2/2m \pm \beta|\boldsymbol{h}_{\boldsymbol{k}}|$, have cubic symmetry.

We find that, for both models, Eqs. (15) and (16), the susceptibilities and Hall coefficients are corrected by terms of order $\beta^2$

$$\chi_{\mathsf{CSR}} = \frac{e^2}{m}(n + \beta^2 \Delta\chi_{\mathsf{CSR}}), \qquad R_H = \frac{1 + \beta^2 \mathcal{K}(n)}{nec}. \quad (17)$$

The results for the corrections of both Eq. (15) and Eq. (16) are listed in Table II. The density dependence and sign of the intraband corrections for the heavy holes model (15) are consistent with Ref. [10]. Our new results for the interband regime [15] show that, while $\chi^{\mathsf{INTER}}_{\mathsf{CMC}} = \chi^{\mathsf{INTRA}}_{\mathsf{CMC}}$, the sum rule is different since it acquires no order $\beta^2$ corrections, i.e., $\chi^{\mathsf{INTER}}_{\mathsf{CSR}} = (e^2 n/m)$. As a result, we obtain that $\mathcal{K}^{\mathsf{INTER}} = -\mathcal{K}^{\mathsf{INTRA}}$, that is to say, the spin-orbit correction to the Drude Hall coefficient reverses sign as disorder increases between the intraband and interband scattering regimes.

TABLE II. Spin-orbit corrections to the sum rule and Hall coefficient factor for the two dimensional hole bands Eq. (15), and three dimensional conduction bands, Eq. (16). Results for the intraband and interband transport regimes are displayed. The conductivity sum rule receives no order $\beta^2$ correction in the interband regime.

| Model | $\Delta\chi^{\mathsf{INTRA}}_{\mathsf{CSR}}/m^2$ | $\mathcal{K}^{\mathsf{INTRA}}/m^2$ | $\mathcal{K}^{\mathsf{INTER}}/m^2$ |
|---|---|---|---|
| 2D$H$ | $-18\pi n^2$ | $18\pi n$ | $-18\pi n$ |
| 3D$C$ | $-8.0(1)n^{5/3}$ | $-17.5(1)n^{2/3}$ | $-23.0(1)n^{2/3}$ |

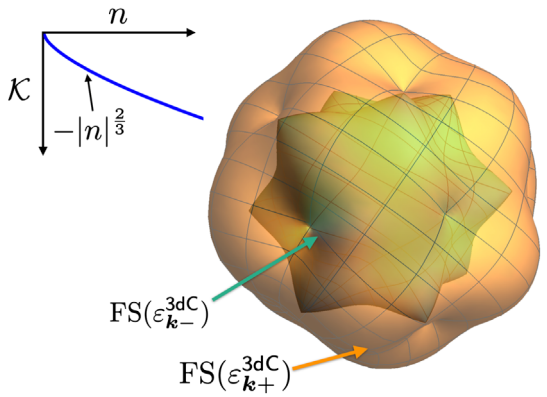


FIG. 3. Spin-orbit split Fermi surfaces (FS) of conduction electrons described by the Hamiltonian Eq. (16). Top left: Density dependence of the non-Drude correction $\mathcal{K}$, Eq. (17).

For $h^{3DC}(\boldsymbol{k})$, the spin-orbit correction $\Delta\chi^{3DC}_{\mathsf{CSR}}$ is of order $-n^{5/3}$ due to the $k^3$ scaling of $\boldsymbol{h}(\boldsymbol{k})$. The interband susceptibility $\chi^{\mathsf{INTER}}_{\mathsf{CMC}}$ is not equal in magnitude to $\chi^{\mathsf{INTRA}}_{\mathsf{CMC}}$, which appears to be due to nonspherical symmetry of the band structure, as shown in Fig. 3.

*Estimation of the correction $\mathcal{R}^{\mathrm{corr}}$.*—Now, we prove that $\mathcal{R}^{\mathrm{corr}}$, of Eq. (3), vanishes as (at least) two powers of the disorder potential over the Fermi energy. Explicit instructions to calculate the moments, recurrents, Krylov bases, and magnetization matrix elements [14] are reviewed in [15]. First. let us consider the intraband scattering regime where $V_{\mathrm{dis}} \ll \Delta\varepsilon \ll \varepsilon_F$.

The intraband currents commute with the clean Hamiltonian $[\mathcal{H}_0, j^{\alpha}_{\mathsf{INTRA}}{}^{x}] = 0$. Hence, the high order Krylov operators are produced by commuting the current with at least one power of the disorder potential. Therefore, the magnetization matrix elements between normalized Krylov bases should scale as

$$(1 - \delta_{i,0}\delta_{j,0})|\mathcal{M}''_{2i,2j}| \propto \frac{\chi_{\mathsf{CMC}}}{\chi_{\mathsf{CSR}}}\left[\frac{V_{\mathrm{dis}}}{\varepsilon_F} + \mathcal{O}\left(\frac{V_{\mathrm{dis}}}{\varepsilon_F}\right)^2\right]. \quad (18)$$

For similar reasons, the first two conductivity moments scale as

$$\mu_2 \propto \chi_{\mathsf{CSR}} V^2_{\mathrm{dis}},$$
$$\mu_4 \propto \chi_{\mathsf{CSR}}[\varepsilon_F^2 V^2_{\mathrm{dis}} + \mathcal{O}(V^4_{\mathrm{dis}})]. \quad (19)$$

Transforming moments to recurrents (see [15]) yields the ratio

$$\frac{\Delta_1}{\Delta_2} = \left(\frac{\mu_2^2}{\chi_{\mathsf{CSR}}\mu_4 - \mu_2^2}\right)^{\frac{1}{2}} \propto \frac{V_{\mathrm{dis}}}{\varepsilon_F}. \quad (20)$$

Combining (18) and (20) in (3), we obtain an overall multiplicative factor

$$|\mathcal{R}^{\rm corr}| \propto \frac{|\chi_{\rm CMC}|}{\chi^2_{\rm CSR}}\left(\frac{V^2_{\rm dis}}{\varepsilon^2_F}\right). \tag{21}$$

In the metallic phase, $R_H, \chi_{\rm CMC}/(\chi_{\rm CSR})^2 < \infty$, and hence, the infinite sum in $\mathcal{R}^{\rm corr}$ must converge. Therefore, the coefficient of proportionality in (21) must be finite.

For the interband regime, we use Eqs. (4), (7) to obtain $\mu_2 = ||\,[\mathcal{H}, j^x]\,||^2 \propto [V^2_{\rm dis} + (\Delta\varepsilon)^2]\chi_{\rm CSR}$. We also assume $(\Delta\varepsilon)^2 \le V^2_{\rm dis}$. Thus, we can appeal again to Eqs. (18), (20) by simply replacing $V^2_{\rm dis} \to V^2_{\rm dis} + (\Delta\varepsilon)^2 \le 2V^2_{\rm dis}$. This recovers the same proportionality if Eq. (21) is also applicable to the interband regime, where we use $\chi^{\rm INTER}_{\rm CMC}/(\chi^{\rm INTER}_{\rm CSR})^2$ to compute the Hall coefficient [29]. Thus, $\mathcal{R}^{\rm corr}$ can be neglected relative to the ratio of corresponding susceptibilities as long as $V^2_{\rm dis} \ll \varepsilon^2_F$ in both intraband and interband regimes.

*Summary.*—Equation (1) provides insight into deviations from Drude's relation in semimetals. Our calculations demonstrate the effects of nonspherical and multiple Fermi surfaces, and interband scattering. These effects should be considered when comparing the "Hall number" ($R_H^{-1}$) to the Fermi volume, as determined by, e.g., angular resolved photoemission [2] and magnetotransport oscillations [30,31]. For time reversal invariant Weyl semimetals, topologically protected surface states have been shown [32] to contribute substantially to the longitudinal conductivity in small samples. Future investigations of the finite size corrections to the Hall coefficient due to surface Fermi arc states would be interesting. For graphene, we propose to split the Dirac cones by an in plane magnetic field. The Hall coefficient should vanish between gate voltages $V_{\rm gate} = \pm g\mu_B B/e$, which may enable measurements of the compressibility at low densities.

We acknowledge support from the US-Israel Binational Science Foundation Grant No. 2016168 and the Israel Science Foundation Grant No. 2021367. This research was also supported in part by the ICTS/topmatter2019/12 Program and the program at KITP Santa Barbara, funded by the National Science Foundation under Grant No. NSF PHY-1748958.

*abhiseks@campus.technion.ac.il
†darovas@ucsd.edu
‡assa@physics.technion.ac.il

[1] H. Zhang, C.-X. Liu, X.-L. Qi, X. Dai, Z. Fang, and S.-C. Zhang, Topological insulators in $Bi_2Se_3$, $Bi_2Te_3$ and $Sb_2Te_3$ with a single Dirac cone on the surface, Nat. Phys. **5**, 438 (2009).

[2] Y. Xia, D. Qian, D. Hsieh, L. Wray, A. Pal, H. Lin, A. Bansil, D. Grauer, Y. S. Hor, R. J. Cava *et al.*, Observation of a large-gap topological-insulator class with a single Dirac cone on the surface, Nat. Phys. **5**, 398 (2009).

[3] Y. Wu, L.-L. Wang, E. Mun, D. D Johnson, D. Mou, L. Huang, Y. Lee, S. L. Budko, P. C. Canfield, and A. Kaminski, Dirac node arcs in $PtSn_4$, Nat. Phys. **12**, 667 (2016).

[4] S.-Y. Xu *et al.*, Discovery of a Weyl fermion semimetal and topological Fermi arcs, Science **349**, 613 (2015).

[5] X. Wan, A. M Turner, A. Vishwanath, and S. Y Savrasov, Topological semimetal and Fermi-arc surface states in the electronic structure of pyrochlore iridates, Phys. Rev. B **83**, 205101 (2011).

[6] A. A. Burkov, M. D. Hook, and L. Balents, Topological nodal semimetals, Phys. Rev. B **84**, 235126 (2011).

[7] T. Bzdušek, Q. S. Wu, A. Rüegg, M. Sigrist, and A. A Soluyanov, Nodal-chain metals, Nature (London) **538**, 75 (2016).

[8] Y. Wu, L.-L. Wang, E. Mun, D. D Johnson, D. Mou, L. Huang, Y. Lee, S. L Budako, P. C Canfield, and A. Kaminski, Dirac node arcs in $PtSn_4$, Nat. Phys. **12**, 667 (2016).

[9] X.-L. Qi and S.-C. Zhang, Topological insulators and superconductors, Rev. Mod. Phys. **83**, 1057 (2011).

[10] H. Liu, E. Marcellina, A. R. Hamilton, and D. Culcer, Strong Spin-Orbit Contribution to the Hall Coefficient of Two-Dimensional Hole Systems, Phys. Rev. Lett. **121**, 087701 (2018).

[11] P. B. Allen and B. Chakraborty, Infrared and dc conductivity in metals with strong scattering: nonclassical behavior from a generalized Boltzmann equation containing band-mixing effects, Phys. Rev. B **23**, 4815 (1981).

[12] A. Auerbach and P. B Allen, Universal high-temperature saturation in phonon and electron transport, Phys. Rev. B **29**, 2884 (1984).

[13] A. Auerbach, Hall Number of Strongly Correlated Metals, Phys. Rev. Lett. **121**, 066601 (2018).

[14] A. Auerbach, Equilibrium formulae for transverse magneto-transport of strongly correlated metals, Phys. Rev. B **99**, 115115 (2019).

[15] Supplemental Material at http://link.aps.org/supplemental/10.1103/PhysRevLett.126.076603 reviews the calculation of current cross susceptibilities and conductivity recurrents. It also includes the detailed derivation of current-magnetization-current and conductivity sum rule susceptibilities ($\chi_{\rm CMC}$ and $\chi_{\rm CSR}$) for the models which are studied in the main text.

[16] N. H. Lindner and A. Auerbach, Conductivity of hard core bosons: A paradigm of a bad metal, Phys. Rev. B **81**, 054512 (2010).

[17] Drude's relation $R_H = (nec)^{-1}$ also holds for elliptical bands $\varepsilon(\boldsymbol{k}) = \varepsilon[\sqrt{\sum_{i=1}^{d}(a_\alpha k_\alpha)^2}]$, for any $\{a_\alpha\}$.

[18] J. M. Ziman, *Electrons and Phonons: The Theory of Transport Phenomena in Solids* (Oxford University Press, New York, 2001).

[19] All perturbations to the band Hamiltonian, including those which give rise to anisotropic $\boldsymbol{k}$-dependent scattering rates, contribute only to $R^{\rm corr}$ which, by Eq. (21), vanishes for weak disorder.

[20] T. Hazra, N. Verma, and M. Randeria, Bounds on the Superconducting Transition Temperature: Applications to Twisted Bilayer Graphene and Cold Atoms, Phys. Rev. X **9**, 031049 (2019).

[21] A tilted Weyl cone model includes an additional $\boldsymbol{u}\cdot\boldsymbol{k}\mathbb{I}$ which, for large $|\boldsymbol{u}|$, defines a type-II Weyl semimetal [33],

with large electron and hole pockets at the Weyl point filling. For $0 < |\boldsymbol{u}| < 1$, $R_H$ is evaluated in [15].

[22] A. H. C. Neto, F. Guinea, N. M. R. Peres, K. S. Novoselov, and A. K. Geim, The electronic properties of graphene, Rev. Mod. Phys. **81**, 109 (2009).

[23] C. Fang, H. Weng, X. Dai, and Z. Fang, Topological nodal line semimetals, Chin. Phys. B **25**, 117106 (2016).

[24] Y. Shao, A. N. Rudenko, J. Hu, Z. Sun, Y. Zhu, S. Moon, A. J. Millis, S. Yuan, A. I. Lichtenstein, D. Smirnov, Z. Q. Mao, M. I. Katsnelson, and D. N. Basov, Electronic correlations in nodal-line semimetals, Nat. Phys. **16**, 636 (2020).

[25] B. Song, C. He, S. Niu, L. Zhang, Z. Ren, X.-J. Liu, and G.-B. Jo, Observation of nodal-line semimetal with ultracold fermions in an optical lattice, Nat. Phys. **15**, 911 (2019).

[26] E. O. Kane, Band structure of indium antimonide, J. Phys. Chem. Solids **1**, 249 (1957).

[27] J. M. Luttinger, Quantum theory of cyclotron resonance in semiconductors: General theory, Phys. Rev. **102**, 1030 (1956).

[28] R. Winkler, Spin-orbit coupling effects in two-dimensional electron and hole systems, Springer Tracts Mod. Phys. **191**, 1 (2003).

[29] It is not advisable to use $\chi^{\mathrm{INTER}}_{\mathrm{CMC}}$, $\chi^{\mathrm{INTER}}_{\mathrm{CSR}}$ in the intraband scattering regime. The commutator of the Hamiltonian with the interband current $j^{x}_{12}(\boldsymbol{k})$ produces a correction $\mathcal{R}^{\mathrm{corr}} \propto (\Delta\varepsilon)^2$, which does not vanish in the zero disorder limit. The use of the projected intraband current ensures that the correction vanishes at weak disorder.

[30] D.-X. Qu, Y. S. Hor, J. Xiong, R. J. Cava, and N. P. Ong, Quantum oscillations and Hall anomaly of surface states in the topological insulator $Bi_2Te_3$, Science **329**, 821 (2010).

[31] C. Bergemann, S. R. Julian, A. P. Mackenzie, S. NishiZaki, and Y. Maeno, Detailed Topography of the Fermi Surface of $Sr_2RuO_4$, Phys. Rev. Lett. **84**, 2662 (2000).

[32] M. Breitkreiz and P. W. Brouwer, Large Contribution of Fermi Arcs to the Conductivity of Topological Metals, Phys. Rev. Lett. **123**, 066804 (2019).

[33] A. A. Soluyanov, D. Gresch, Z. Wang, Q. S. Wu, M. Troyer, and B. A. Bernevig, Type-II Weyl semimetals, Nature (London) **527**, 495 (2015).